The Plant Cell, Vol. 19: 1081–1095, March 2007, www.plantcell.org

Death Don't Have No Mercy and Neither Does Calcium: *Arabidopsis* CYCLIC NUCLEOTIDE GATED CHANNEL2 and Innate Immunity [W]

Rashid Ali, Wei Ma, Fouad Lemtiri-Chlieh, Dimitrios Tsaltas, Qiang Leng, Susannne von Bodman, and Gerald A. Berkowitz[1]

Agricultural Biotechnology Laboratory, University of Connecticut, Storrs, Connecticut 06269-4163

Plant innate immune response to pathogen infection includes an elegant signaling pathway leading to reactive oxygen species generation and resulting hypersensitive response (HR); localized programmed cell death in tissue surrounding the initial infection site limits pathogen spread. A veritable symphony of cytosolic signaling molecules (including Ca^{2+}, nitric oxide [NO], cyclic nucleotides, and calmodulin) have been suggested as early components of HR signaling. However, specific interactions among these cytosolic secondary messengers and their roles in the signal cascade are still unclear. Here, we report some aspects of how plants translate perception of a pathogen into a signal cascade leading to an innate immune response. We show that *Arabidopsis thaliana* CYCLIC NUCLEOTIDE GATED CHANNEL2 (CNGC2/DND1) conducts Ca^{2+} into cells and provide a model linking this Ca^{2+} current to downstream NO production. NO is a critical signaling molecule invoking plant innate immune response to pathogens. Plants without functional CNGC2 lack this cell membrane Ca^{2+} current and do not display HR; providing the mutant with NO complements this phenotype. The bacterial pathogen–associated molecular pattern elicitor lipopolysaccharide activates a CNGC Ca^{2+} current, which may be linked to NO generation due to buildup of cytosolic Ca^{2+}/calmodulin.

INTRODUCTION

Plants have an innate immune response to bacterial infection similar in some ways to that of animals (Nürnberger et al., 2004). One component of plant innate immunity is localized plant cell apoptosis; necrotic lesions formed around the initial site of infection limit pathogen spread. A decade ago, in an article entitled "Death Don't Have No Mercy," Dangl et al. (1996) reviewed the steps involved in this plant programmed cell death/hypersensitive response (HR) to avirulent pathogens, indicating that cell membrane Ca^{2+} flux occurs early in this signaling pathway. Subsequently, Dangl referred to the signaling molecule nitric oxide (NO) as the "concert master" in HR and plant innate immunity (Dangl, 1998). Since this time, the role of NO in plant signaling has been an active area of investigation (Romero-Puertas et al., 2004; Wendehenne et al., 2004; Crawford and Guo, 2005; Delledonne, 2005; Lamotte et al., 2005). However, the specific gene product facilitating HR-related inward Ca^{2+} currents is unknown, as is the mechanism by which these Ca^{2+} currents are transduced into a rise in NO.

The production of reactive oxygen species (ROS) is involved in HR as an early plant response to initial pathogen perception and rise in cytosolic [Ca^{2+}] (Grant et al., 2000). ROS generation is associated with HR-related apoptosis. ROS interacts with NO to potentiate HR to pathogens (Torres et al., 2006), and the ratio of specific ROS forms and NO act in HR signaling (Delledonne et al., 2001). Furthermore, some evidence suggests Ca^{2+} flux into plant cells occurs both upstream and downstream from ROS generation during plant innate immune response to pathogens (reviewed in Torres et al., 2006).

Little is known in general about the channels that facilitate Ca^{2+} flux into the plant cell. No specific ion channel gene product has yet been associated with Ca^{2+} uptake into plants (White et al., 2002; White and Broadley, 2003). One homolog (CNGC2) of the large (20 members in *Arabidopsis thaliana*) family of cyclic nucleotide gated channels (CNGCs) has been shown to conduct Ca^{2+} and K^+ when expressed in heterologous systems (Leng et al., 1999, 2002; Hua et al., 2003a, 2003b). Recent reviews suggest that CNGCs may be involved in Ca^{2+} uptake into plants (White et al., 2002) and plasma membrane Ca^{2+} currents associated with signal transduction cascades (Hetherington and Brownlee, 2004). However, we know little about the molecular architecture of native channels comprised of CNGC subunits. Animal homologs of plant CNGCs are heterotetramers formed from at least two (Flynn et al., 2001), and in many cases three (e.g., Zheng and Zagotta, 2004), different CNGC gene translation products. Computational molecular modeling of the quaternary structure of channels formed by CNGC2 (and other plant CNGC) polypeptides suggests that plant CNGCs also function as tetramers (Hua et al., 2003a); it is unknown whether or not plant CNGCs are heteromeric. Furthermore, publicly accessible expression profiling databases (e.g., see Talke et al., 2003) indicate

[1] To whom correspondence should be addressed. E-mail gerald.berkowitz@uconn.edu; fax 860-486-0534.
The author responsible for distribution of materials integral to the findings presented in this article in accordance with the policy described in the Instructions for Authors (www.plantcell.org) is: Gerald A. Berkowitz (gerald.berkowitz@uconn.edu).
[W] Online version contains Web-only data.
www.plantcell.org/cgi/doi/10.1105/tpc.106.045096

that many or most of the plant CNGCs (including CNGC2) have overlapping expression profiles. Therefore, it is at present unclear whether or not translational arrest of one plant CNGC would alter conductance properties across native plant cell membranes.

An Arg-dependent nitric oxide synthase (NOS) enzyme catalyzes HR-related NO generation in plants (Delledonne et al., 1998; Durner et al., 1998). A gene encoding a plant NOS enzyme has not yet been identified and/or cloned (Crawford et al., 2006; Zemojtel et al., 2006). However, analysis of a loss-of-function *Arabidopsis* mutant has demonstrated the involvement of the *Arabidopsis NITRIC OXIDE ASSOCIATED PROTEIN1* (*NOA1*; formerly named At *NOS1*) translation product in a pathway leading to Arg-dependent NO generation (Guo et al., 2003) and implicated this gene product in signal cascades responding to pathogen infection of plants (Zeidler et al., 2004; Crawford and Guo, 2005). Loss-of-function At *noa1* mutants have reduced basal NO levels and reductions in signaling-associated NO generation (Zeidler et al., 2004; Bright et al., 2006; Zhao et al., 2006). NO activates nucleotide cyclases in plants and animals (Durner et al., 1998); recent reviews (Wendehenne et al., 2001; Delledonne, 2005) therefore place cyclic nucleotide monophosphate rise downstream from NO generation in HR signaling. Here, we use the *defense no death1* (*dnd1*) *Arabidopsis* mutant (Clough et al., 2000) that has a null mutation in the *CNGC2/DND1* gene and displays no HR to link cyclic nucleotide monophosphate–dependent Ca^{2+} flux to NO generation and HR of plants to pathogen infection.

RESULTS AND DISCUSSION

NO Involvement in Plant Pathogen Signaling

Much evidence implicates NO as involved in the HR response to pathogens (for reviews, see Wendehenne et al., 2001, 2004; Romero-Puertas et al., 2004; Delledonne, 2005; Lamotte et al., 2005). Particularly compelling support for NO involvement in HR signaling is the demonstration that inhibitors of enzymatic NO synthesis block HR in *Arabidopsis* leaves inoculated with an avirulent pathogen (Delledonne et al., 1998). However, whether or not NO generation is causal to and/or required for the HR response to pathogens is still unclear. Some evidence specifically indicates that in *Arabidopsis*, NO may not be involved as a signaling component controlling HR, but rather acts to facilitate cell-to-cell spread of the HR at the infection site and temporally potentiate HR response to pathogens (Zhang et al., 2003).

We used the *Arabidopsis dnd1* mutant, which lacks a functional cyclic nucleotide gated channel (CNGC2) and also displays no classic HR to avirulent pathogens (Clough et al., 2000), to further characterize the role of NO in the HR response of *Arabidopsis*. Guo et al. (2003) used application (to the growing medium) of the NO donor sodium nitroprusside (SNP) to revert some At *noa1* (formally, At *nos1*) mutant phenotypes to the wild type. More recently, Bright et al. (2006) and Zhao et al. (2006) also reverted some *At noa1* mutant phenotypes to the wild type using SNP application. Here, we demonstrated that addition of SNP to *dnd1* plants in a similar manner partially overcomes the lack of HR response to the avirulent bacterial pathogen *Pseudomonas syringae* (Figure 1). Pictures of representative (*Arabidopsis* wild-type and *dnd1*) leaves inoculated with *P. syringae* pv *syringae* (*Pss*) from one experiment are shown in Figure 1B (also see Figure 1D). Quantified evaluations of HR development and concomitant tissue collapse using a standard HR scoring system (see Methods) from the same experiment are shown in Figure 1C. Ethanol bleaching has been used as a convenient assay to provide enhanced visualization of HR development in leaves responding to an avirulent pathogen (Schornack et al., 2004; Weber et al., 2005). HR development and tissue collapse in leaves of *dnd1* plants pretreated with SNP and inoculated with *Pss* were visualized in another experiment (with a different set of plants) after ethanol bleaching (Figure 1E). Additional experiments were undertaken with another *P. syringae* pathovar, *P. syringae* pv *tomato* DC3000 (*Pst*), containing the avirulence gene *avrRpt2*. As was the case with *Pss*, *dnd1* plants did not undergo HR when inoculated with *Pst avrRpt2*$^+$, and pretreatment with SNP complemented this phenotype. In this experiment, SNP effects on *dnd1* leaves were demonstrated after ethanol bleaching; Figure 1F shows the tissue collapse evident in *dnd1* leaves inoculated with *Pst avrRpt2*$^+$ only upon pretreatment with SNP. Yu et al. (1998) used autofluorescense of tissue undergoing apoptosis to document the absence of HR response to *Pst avrRpt2*$^+$ in *dnd1* leaves. We used a similar assay to further evaluate the effect of SNP on HR in *dnd1* leaves inoculated with *Pst avrRpt2*$^+$. In their work, Yu et al. (1998) observed autofluorescence associated with confluent cell apoptosis at the edge of the inoculation zone in wild-type leaves that was absent in *dnd1* leaves. Measurement of autofluorescence at the edge of the inoculation zone in *dnd1* leaves shows evidence of HR only when plants were pretreated with SNP (Figure 1G); the −SNP image is similar to that shown by Yu et al. (1998) for *dnd1*. Addition of SNP has no apparent effect on the wild-type HR response to *Pss* (Figures 1B and 1C). Treatment of wild-type and *dnd1* plants with SNP in the absence of pathogen infection did not induce any observable HR symptoms (Figure 1A; data not shown).

Results shown in Figure 1 indicate that the lack of NO generation in the *dnd1* mutant is causal to the block of signaling leading to HR. Furthermore, these results are consistent with the assertion that in *Arabidopsis*, NO generation is required, but not sufficient, for the signaling pathway leading to HR. These studies provide new genetic evidence for a role of NO in the plant HR to pathogens. Application of SNP to *dnd1* plants only partially restores HR. We speculate that this could be due to either (1) the possibility that artificially generating NO in plants by application of SNP does not completely mimic the situation in wild-type plants responding to avirulent pathogens (*Pss* or *Pst avrRpt2*$^+$) in terms of the level and/or specific site of NO accumulation, or (2) other unknown factors contribute to block of HR generation in *dnd1* plants responding to infection with avirulent pathogen.

Lipopolysaccharide, NO, and Ca^{2+} Signaling

In the study reporting the cloning of *At NOA1*, Guo et al. (2003) used the *Arabidopsis* guard cell as a model system to demonstrate the role of NOS (i.e., using Arg as substrate in contrast with nitrite-dependent NO generation) in signal transduction pathways. Their studies employed the NO-specific fluorescent dye

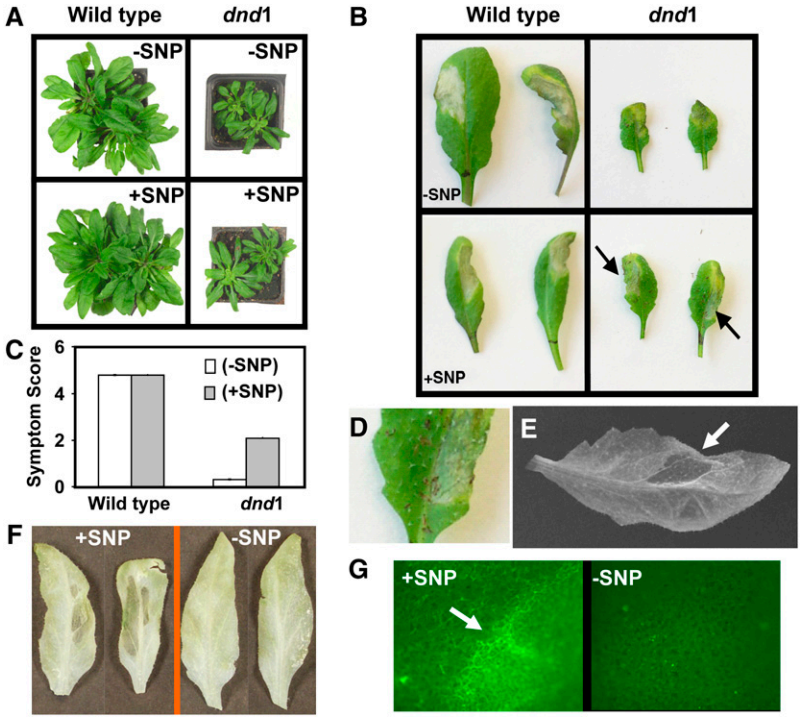

Figure 1. Application of SNP Reverses the Lack of HR of *dnd1* Plants to Infection with Avirulent Pathogen.

(A) Application of SNP in the absence of pathogen had no effect on the wild-type or *dnd1* plant phenotype. Wild-type *Arabidopsis* plants are shown on the left, and *dnd1* plants are shown on the right. The top two panels show 8-week-old plants grown in the absence of SNP. The bottom two panels show plants grown as above for 6 weeks and then irrigated for 2 weeks with solutions containing 100 μM SNP.

(B) Photographs of representative leaves detached from wild-type (left panels) and *dnd1* (right panels) plants 24 h after inoculation with *Pss*. Plants were grown either in the absence (top panels) or presence (bottom panels; irrigation for 2 weeks as in **[A]**) of SNP. Arrows indicate necrotic regions of *dnd1* leaves undergoing HR.

(C) Quantitative scoring of HR in leaves of wild-type and *dnd1* plants inoculated with *Pss* either in the absence (open bars) or presence (closed bars) of SNP. Results are presented as means of a minimum of 25 leaves per treatment ± SE.

(D) Enlarged image of a portion of a (+SNP) *dnd1* leaf shown in the bottom right panel of **(B)** highlighting the region inoculated with *Pss*; note the flattened region undergoing tissue collapse.

(E) A leaf (representative of three replicate treatments) from a *dnd1* plant pretreated with SNP and inoculated with *Pss*. Leaves were removed from plants 48 h after treatment and bleached in ethanol. An arrow indicates the inoculated region, which appears more transparent and flattened compared with the rest of the leaf (also see leaves in **[F]**). This experiment was repeated a total of four times. Representative results from one of these experiments are shown in **(A)** to **(D)**, and results from a different experiment are shown in **(E)**.

(F) Ethanol-bleached *dnd1* leaves excised 9 h after inoculation with *Pst avrRpt2*$^{+}$. Leaves shown in the left panel are from plants pretreated with SNP (as above); the panel on the right shows leaves from *dnd1* plants treated with water.

(G) Prior to ethanol bleaching, autofluorescence of leaves shown in **(F)** was evaluated as described by Balagué et al. (2003). The leaf shown in the left panel is from an SNP-pretreated plant; the leaf in the right panel is from a *dnd1* plant treated with water. Regions at the edge of the inoculation zone are shown in both cases. We are aware that leaf veins display spontaneous autofluorescense; only interveinal regions are shown for +SNP and −SNP leaves. The arrow indicates autofluorescense occurring at the edge of the inoculation zone in *dnd1* plants pretreated with SNP. A similar region of the inoculation zone was imaged for −SNP plants. Other experiments (data not shown) indicated that pretreatment of wild-type plants with SNP did not affect the HR response to *Pst avrRpt2*$^{+}$ and that wild-type plants display no HR response to *Pst avrRpt2*$^{-}$.

diaminofluorescein diacetate (DAF-2DA) to monitor NO generation in vivo. Application of the dye along with various effectors/inhibitors to leaf epidermal peels with exposed, intact guard cells allows for real-time observation of NO generation in a cell responding to an external stimulus (Guo et al., 2003). Here, we followed a similar approach to elucidate components of the signaling pathway leading to NO generation in plants responding to pathogen infection. It should be noted that guard cells have been previously shown to display classic innate immune response to both pathogen-associated molecular pattern (PAMP) compounds and pathogens (Lee et al., 1999; Wright et al., 2000), justifying our use of this model system here.

We compared NO generation in guard cells isolated from wild-type and *dnd1* plants upon application of lipopolysaccharide (LPS). LPS is a ubiquitous component of Gram-negative bacteria, including *P. syringae* (Zeidler et al., 2004). Molecules such as LPS are elicitors of plant (and animal) innate immune response and as such are known as PAMPs (Nürnberger et al., 2004; Delledonne, 2005). LPS has recently been shown to induce a burst of NOS-dependent (i.e., Arg) NO generation in *Arabidopsis* (suspension

cells and epidermal peels) (Zeidler et al., 2004). LPS has been shown to induce a cytosolic Ca^{2+} spike and associated oxidative burst in tobacco (*Nicotiana tabacum*) cells (Braun et al., 2005) and potentiate expression of plant defense mechanisms responding to pathogen infection in pepper (*Capsicum annuum*) leaves (Newman et al., 2002). These studies, then, support the rationale of using LPS to probe the signal cascade leading to pathogen-induced NO generation. It should be noted that no studies to date have linked LPS application in the absence of a pathogen to HR in *Arabidopsis*. However, the focus of our work is to probe the signaling pathway leading to NO generation. Clearly, generation of NO alone does not lead to HR; as mentioned above, we observed no HR symptoms in wild-type or *dnd1* plants when SNP was supplied in the absence of the avirulent pathogen (Figure 1A).

It should be noted that our assay of NO generation within intact cells (i.e., monitoring fluorescence changes of an NO-specific dye) is indirect. However, the use of this experimental approach was calibrated by Zeidler et al. (2004) with a direct NO assay. They found that whether NO was quantified directly using electron paramagnetic resonance imaging with Fe_2 and diethyldithiocarbamate as a spin trap, or indirectly using the dye DAF-2DA as we do here, LPS similarly caused NO generation in *Arabidopsis* cells. Recent work by Planchet and Kaiser (2006) also supports the efficacy of DAF-2DA measurement of NO production by plant cells. As shown in Figure 2, LPS application evokes NO generation in guard cells of wild-type plants, and this response is inhibited in *dnd1* guard cells (cf. Figures 2A and 2B); this result is consistent with the Ca^{2+}-conducting channel CNGC2 as involved with elicitor/PAMP-dependent NO generation and, presumably, plant innate immune response to pathogens. Our observations regarding LPS and NO generation were done using epidermal peels, similar to the studies of Guo et al. (2003) and Zeidler et al. (2004). Epidermal peels of *Arabidopsis* leaves typically do not contain intact mesophyll cells, but guard cells are present and viable (Guo et al., 2003). In our use of this model system, we do not imply that our observations are necessarily exclusive to guard cells. Inhibition of NO generation is not due to a lack of dye loading in the cells of the mutant. Incubation in solutions containing the NO donor SNP resulted in dye fluorescence in the wild-type and *dnd1* guard cells, demonstrating a functional assay for NO presence in both cases (Figure 2C). For experiments involving use of DAF-2DA fluorescence to monitor NO generation, results are presented (in Figures 2 and 3) as images representative of at least three replicates. Quantification of treatment means for NO generation in these experiments is shown in Figure 4; treatment differences in the quantification analysis (Figure 4) show similar trends as can be observed in Figures 2 and 3.

There are a number of potential enzymatic (e.g., nitrate reductase and NOS) and nonenzymatic sources of NO generation in plants. Results shown in Figure 3 are consistent with an Arg-dependent (i.e., NOS) pathway as the source of LPS-induced NO in wild-type guard cells, a response inhibited in guard cells prepared from the *dnd1* mutant. LPS-dependent NO generation in wild-type guard cells (Figure 3A) was completely blocked by addition of the NOS inhibitor N^G-nitro-L-Arg-methyl ester (L-NAME) (Figure 3C). No LPS-dependent NO generation was observed in *dnd1* epidermal peels in the presence of L-NAME as well (Figure 3D). The inactive isomer D-NAME had no effect on LPS-dependent NO generation (Figures 3I and 3K). Zeidler et al. (2004) found that LPS-dependent NO generation was inhibited in epidermal peels of *At noa1* mutants; a result consistent with our assertion here that the LPS-dependent NO generation inhibited in *dnd1* epidermal peels occurs through an Arg-dependent NO generation pathway in wild-type tissue.

Prior patch clamp studies from this lab documented the presence of cyclic nucleotide–activated, inward-rectified, Ca^{2+}-conducting channels (such as CNGC2, which is absent from the *dnd1* mutant; see Clough et al., 2000) in the plasma membrane of *Arabidopsis* (and *Vicia faba*) guard cells (Lemtiri-Chlieh and Berkowitz, 2004). In these studies, Gd^{3+} was found to be a potent blocker of this guard cell inward Ca^{2+} current (I_{Ca}). Gd^{3+} has no effect on guard cell K^+ channels at concentrations that effectively

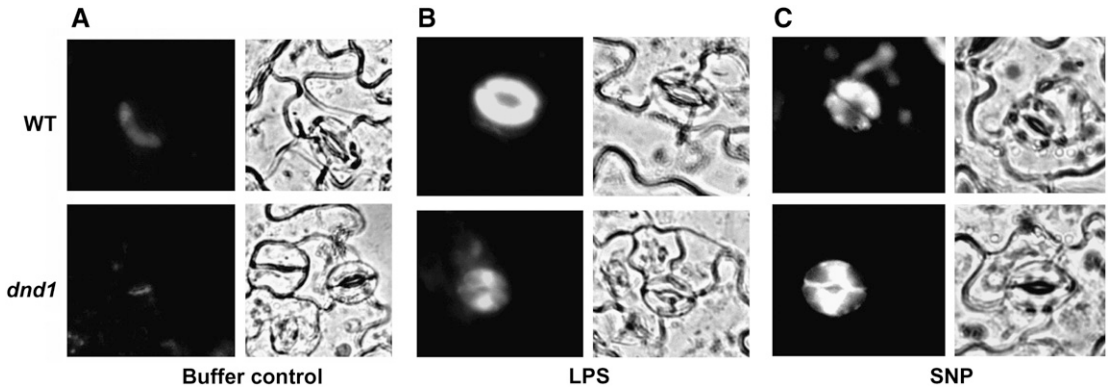

Figure 2. LPS Activation of NO Generation in Wild-Type and *dnd1* Guard Cells.

Leaf epidermal peels prepared from wild-type (top panels) or *dnd1* plants (bottom panels) were loaded with the NO-sensitive dye DAF-2DA prior to incubation in reaction buffer alone (buffer control) **(A)**, 100 μg/mL LPS **(B)**, or 50 μM SNP **(C)**. In each case, corresponding fluorescence and bright-field images are shown; the area of the peel subjected to analysis was greater than that shown in each case. This experiment was repeated a total of three times. Representative cells from one of these experiments are shown. In each experiment, a minimum of three epidermal peels was used as treatment replicates (as was also done for the experiments shown in Figure 3).

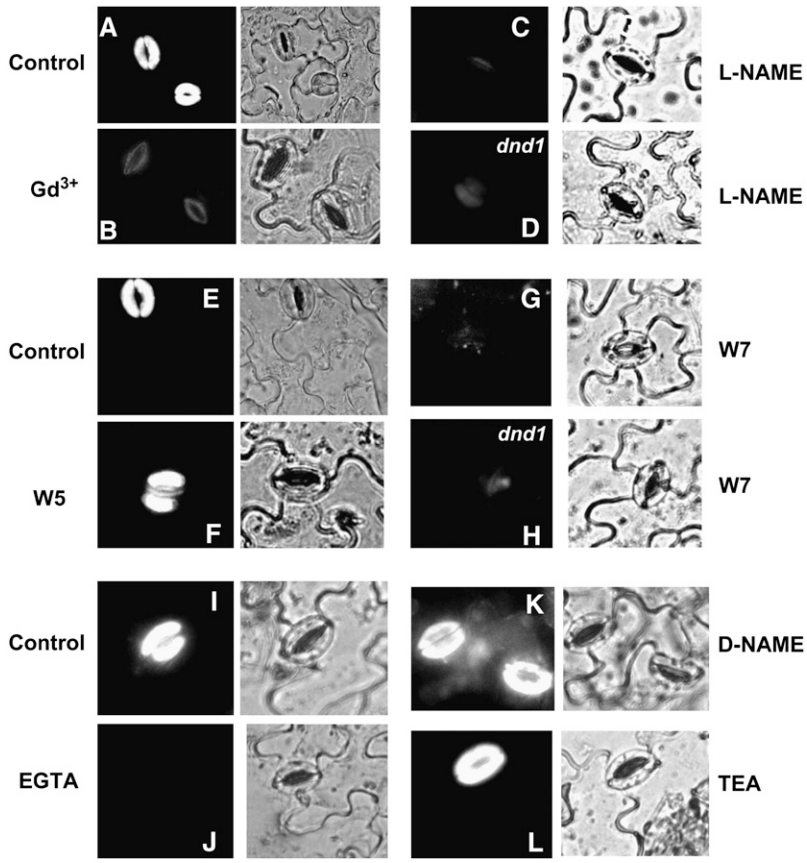

Figure 3. The Signaling Pathway Leading from LPS Perception to NO Generation Involves Ca^{2+}, CAM, and NOS.

LPS activation of NO is blocked by chelation of extracellular Ca^{2+} with 2 mM EGTA **(J)** and by inhibitors of Ca^{2+} channels (100 μM Gd^{3+}; **[B]**), Arg-dependent NOS (200 μM L-NAME; **[C]** and **[D]**), and CaM (50 μM W7; **[G]** and **[H]**). Also shown are results with the W7 analog W5 at 50 μM **(F)**, the L-NAME isomer D-NAME at 200 μM **(K)**, and the K^+ channel blocker TEA at 10 mM **(L)**. In all cases, DAF-2DA was loaded into cells of the epidermal peels and fluorescence was measured after addition of LPS. For each treatment, fluorescence and bright-field images are shown. Results from several experiments are compiled in this figure; controls (i.e., application of LPS alone to wild-type epidermal peels) for each experiment are shown in **(A)**, **(E)**, and **(I)**. Results from epidermal peels prepared from wild-type (**[A]** to **[C]**, **[E]** to **[G]**, and **[I]** to **[L]**) and *dnd1* (**[D]** and **[H]**) plants are shown. Experiments were repeated at least two times; representative images are shown.

block I_{Ca} (Lemtiri-Chlieh et al., 2003). A critical objective of the studies included in this report is to link Ca^{2+} conductance through plasma membrane ion channels to (downstream) generation of NO in a signal cascade. One experimental approach we took to address this research objective was to examine the effects of Gd^{3+} on LPS-activated NO generation in the guard cell. Results shown in Figures 3A and 3B indicate that this Ca^{2+} channel blocker substantially reduces LPS-activated NO generation in wild-type guard cells. By contrast, the K^+-selective channel blocker tetraethylammonium (TEA) had no effect on LPS-activated NO generation (Figures 3I and 3L). Since LPS-activated NO generation is inhibited in *dnd1* guard cells (Figure 2B), the results shown in Figure 3 demonstrating sensitivity of LPS-activated NO generation to Gd^{3+} and insensitivity to TEA in wild-type guard cells are consistent with cell membrane inward Ca^{2+} conductance (through a Gd^{3+}-sensitive CNGC present in wild-type cells) mediating LPS activation of NO. Further evidence that LPS activation of NO generation involves cell membrane Ca^{2+} channels is presented in Figures 3I and 3J; chelation of Ca^{2+} in the reaction solution blocks NO generation. Quantitative analysis of channel blocker, NOS inhibitor, calmodulin (CaM) antagonist, and Ca^{2+} chelator effects on NO generation are shown in Figure 4.

These results, then, link plasma membrane Ca^{2+} conductance to downstream NO generation in *Arabidopsis* cells responding to LPS. Consistent with this conclusion, we find that infiltration of Gd^{3+} into (wild-type) *Arabidopsis* leaves inoculated with *Pss* prevents HR (Figure 5). Drop test assays (see Supplemental Figure 1A online) demonstrate no adverse effect of Gd^{3+} on *Pss* growth, indicating that the effect of Gd^{3+} we find on HR development in the plant (Figure 5) is due to the channel blocker effects on plant signaling as opposed to direct effects on the pathogen.

In a fashion similar to the work shown here, Lamotte et al. (2004) found that the fungal polypeptide elicitor/PAMP cryptogein can induce NO production in *N. tabacum* cell cultures and that this NO generation is blocked by La^{3+} (a Ca^{2+} channel blocker that acts in a fashion similar to Gd^{3+} used here) and by

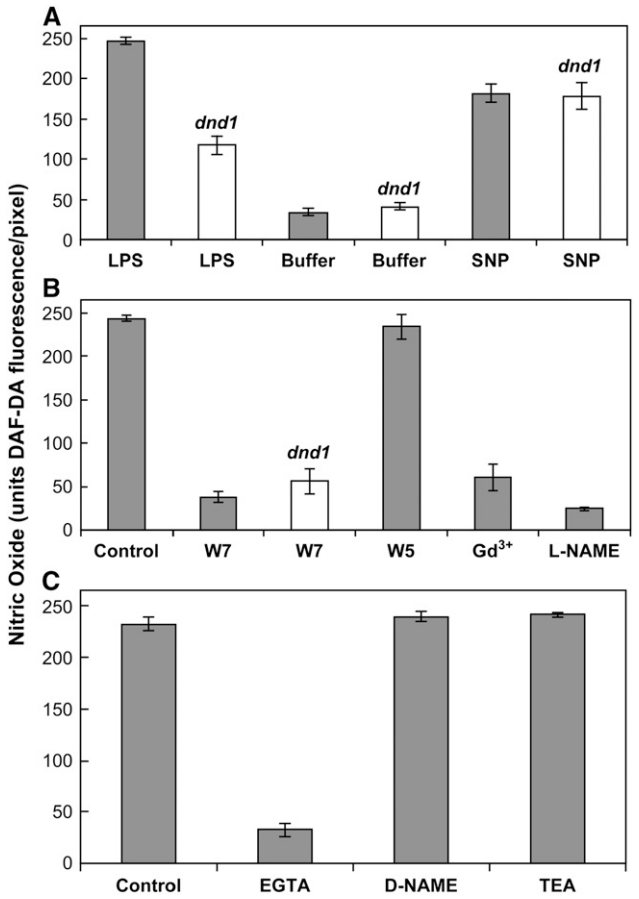

Figure 4. Quantitative Analysis of in Vivo NO Generation Monitored Using DAF-2DA Fluorescence.

The maximum fluorescence intensity that could be measured was 250 units/pixel (see Methods). Results shown are from three independent experiments. Results in **(A)** correspond to images shown in Figure 2; **(B)** and **(C)** correspond to images shown in Figure 3. In all cases, results are presented as mean ($n \geq 3$) fluorescence intensity per pixel (i.e., averaged over the area of a guard cell pair; see Methods) ± SE. In all cases, closed bars represent measurements taken on wild-type tissue; open bars denote measurements of epidermal peels prepared from *dnd1* plants. The experiment shown in **(A)** compares fluorescence intensity of wild-type and *dnd1* guard cells in reaction buffer alone (Buffer), reaction buffer with 100 μg/mL LPS added, or reaction buffer with 50 μM SNP added. For **(B)** and **(C)**, all measurements were undertaken with 100 μg/mL LPS in the reaction solution. Measurements taken with LPS alone added to

EGTA. The important prior work of Lamotte et al. (2004) does identify a link between an elicitor/PAMP, inward Ca^{2+} conductance, and NO similar to the model we develop here. However, the signaling steps mediating cryptogein involvement in HR signal cascades may be somewhat unique. Planchet et al. (2006) recently suggested that cryptogein-mediated NO generation in *N. tabacum* may be mediated by nitrate reductase rather than an Arg-dependent NOS-type enzyme (in contrast with what we find here with LPS; Figure 3) and that the role cryptogein may play in HR might be complex and/or not yet fully characterized (also see Planchet and Kaiser, 2006). We undertook further tests of the Gd^{3+} effect on pathogen-related necrosis beyond that done with *Arabidopsis* shown in Figure 5. Interestingly, we find that infiltration of Gd^{3+} into *N. tabacum* (the same variety, *Xanthi*, used by Planchet et al. [2006] for their in planta studies of cryptogein and NO) blocked HR in plants inoculated with *Pst avrRpm1*$^{+}$ (see Supplemental Figure 1B online). Prior studies have documented that *P. syringae* pv *tomato* (DC3000) causes HR in *N. tabacum* (López-Solanilla et al., 2004). In addition to *Arabidopsis* and *N. tabacum*, we found that Gd^{3+} infiltration blocked pathogen-related necrosis in *V. faba* inoculated with two different pathovars of *P. syringae* as well (see Supplemental Figure 1C online).

Calcium-Permeable Channels and the *dnd1* Mutant

No change in ion conductance profiles has yet been demonstrated in cells of the *dnd1* plant; this mutant has a null mutation in the *CNGC2* gene. As noted in the Introduction, channels formed by CNGC2 alone (i.e., upon expression in heterologous systems) are capable of conducting several different cations. The subunit composition of native plant channels comprised at least in part by the CNGC2 polypeptide is unknown, and more than one type of CNGC may be present in a particular plant membrane, allowing for functional redundancy. Therefore, it cannot be presumed what (or even if a) specific plasma membrane cation conductance would be affected in the *dnd1* mutant. Here, we present patch clamp

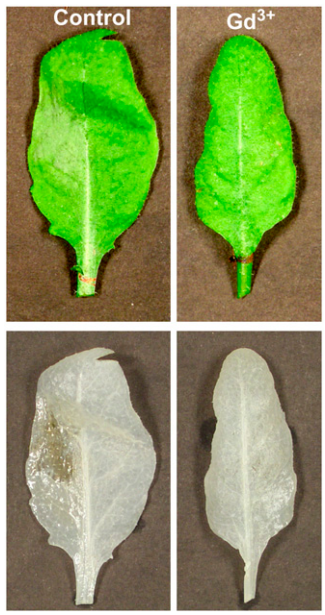

Figure 5. Coinfiltration of a CNGC Ca^{2+} Channel Blocker with Avirulent Pathogen Prevents HR in Wild-Type *Arabidopsis*.

Leaves were inoculated with *Pss* (2×10^8 colony-forming units/mL) alone (control) or *Pss* with 100 μM Gd^{3+}. Photographs were taken after 19 h (top two panels), and then leaves were immersed in ethanol and photographed after 4 d (bottom two panels). Leaves shown are representative of at least three individual inoculations.

recordings from wild-type and *dnd1* guard cell plasma membranes (Figure 6). Studies presented in Figure 6 provide evidence that native plasma membrane ion channel complexes containing CNGC2 are inwardly rectified Ca^{2+}-conducting channels. Application of cAMP to the bath solution activates an inward Ca^{2+} (as is convention, Ba^{2+} is used as the charge carrier in these patch clamp recordings; Gelli and Blumwald, 1997; Peng et al., 2005) current in wild-type *Arabidopsis* guard cell protoplasts. We have characterized this ligand-gated inward Ca^{2+} channel current in guard cell (for characterization of the guard cell Ca^{2+} current, see Lemtiri-Chlieh et al., 2003) and mesophyll cell protoplasts prepared from leaves of wild-type *Arabidopsis* plants previously (Lemtiri-Chlieh and Berkowitz, 2004). In this prior work, the cAMP-activated current was completely blocked by 50 μM Gd^{3+}, and reversal potential (E_{rev}) of currents recorded in the patch configuration was near the Nernst equilibrium potential of Ba^{2+} (E_{Ba}) and far away from E_K and E_{Cl}, evidence consistent with our assertion that the ligand activates a Ca^{2+}-conducting channel. This cAMP-activated current is absent from guard cell protoplasts prepared from leaves of *dnd1* plants (Figure 6).

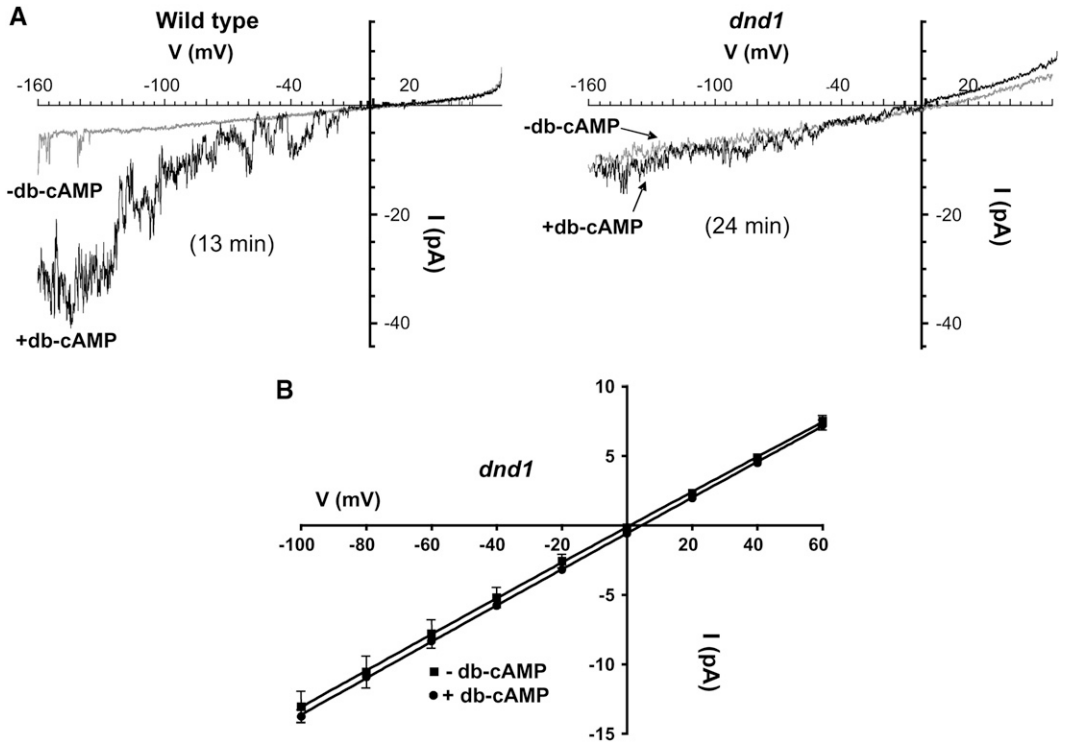

Figure 6. Patch Clamp Analysis Identifies a Cyclic Nucleotide Gated Ca^{2+} Channel in the Plasma Membrane of Guard Cell Protoplasts Prepared from Wild-Type Plants; This Current Is Absent from *dnd1* Guard Cell Protoplasts.

(A) Current/voltage relationships from voltage ramp command protocols recorded in the whole-cell configuration are shown for representative wild-type (left panel) and *dnd1* (right panel) guard cell protoplasts. Current traces from voltage ramps prior to (−db-cAMP; gray current traces) and after (+db-cAMP; black current traces) addition of 1 mM db-cAMP to the perfusion bath are shown. The time period between addition of db-cAMP to the perfusion bath solution and initiation of the voltage ramp shown is noted in parentheses. As described in an earlier publication (Lemtiri-Chlieh and Berkowitz, 2004), this inward Ba^{2+} current is present in wild-type protoplasts in the absence of exogenously added cAMP (e.g., note the flickery channel opening events recorded in the absence of ligand at ~−140 to −160 mV); we speculate that sufficient endogenous cyclic nucleotide may be present in the cell to activate some of the channels present in the membrane. However, when the channel is present in the plasma membrane, we note that adding cyclic nucleotide (at levels used here) always increases the magnitude of the whole-cell current, as is shown here in the case of wild-type protoplasts (Lemtiri-Chlieh and Berkowitz, 2004). Coincident with the dwarf phenotype of *dnd1* plants (Figure 1A) and smaller leaves of the mutant (Figure 1B), we anecdotally note that *dnd1* guard cell protoplasts are smaller than wild-type cells and are extremely difficult to patch. When forming giga-ohm seals with *dnd1* guard cells, the protoplast often is sucked up into the patch pipette. We successfully patched three *dnd1* guard cells (from three different protoplast preparations) for long enough time periods to allow for db-cAMP addition and incubation of the protoplast in activating ligand for >15 min; the recording shown is representative of these three experiments. In all three cases, application of db-cAMP did not increase the inward Ba^{2+} current (see **[B]**). We observed cyclic nucleotide activation of current in wild-type guard cells in 13 of 15 cells tested.

(B) Calculated mean current at various step voltages (±SE) for *dnd1* guard cells in the absence (squares) and presence (circles) of 1 mM db-cAMP ($n = 3$ in both cases). The calculated current/voltage relationship does not appear rectified and reverses at ~0 mV, suggesting that leak current may contribute significantly to the measured values in *dnd1* cells. However, note that the calculated current at each voltage does not appear to be affected by addition of db-cAMP in these cells.

In our prior study of the cAMP effects on the Ca^{2+}-conducting channel in wild-type cells (Lemtiri-Chlieh and Berkowitz, 2004), we noted that inward current in the presence of the activating ligand cAMP was 440% (±28%, $n = 7$) the level recorded in the absence of cAMP at −140 mV. In the recordings shown in Figure 6A, current at this voltage in the presence of cAMP was 480% of the level in the absence of cAMP with the wild-type guard cell (a 380% increase), while current recorded from *dnd1* guard cells with cAMP was 118% of the level measured in the absence of cAMP (i.e., an 18% increase with *dnd1* guard cells). As shown in Figure 6B, mean currents (averaged from the three *dnd1* guard cells tested) showed no significant change associated with cAMP addition over a range of voltages. For example, at −80 mV, the average current recorded from *dnd1* guard cells was −10.6 ± 1.1 pA and −10.9 ± 0.3 pA in the absence and presence of cAMP (Figure 6B).

Results shown in Figure 6 link a specific gene product in plants with the presence of a functional Ca^{2+} channel in a plant cell plasma membrane. This work also provides direct electrophysiological evidence that a specific CNGC isoform is functionally expressed in the plasma membrane of plant cells. Bindschedler et al. (2001) have shown that modulators of cytosolic cAMP levels affect PAMP-induced ROS generation. Thus, results presented here (Figures 1 to 6) are consistent with prior speculations by Bindschedler et al. (2001) about CNGC involvement in a plant innate immunity signal cascade.

Regulation of NO Synthesis: Filling in the Steps of the Signal Transduction Cascade

The studies we report here that link a CNGC2-dependent Ca^{2+} current (Figure 6) to NO generation in the HR signaling cascade (Figures 1 to 5) allow us to further probe the specific steps of this pathogen perception/innate immunity signal transduction pathway. Results shown in Figures 3E to 3H address the question of what molecular mechanism transduces a plasma membrane Ca^{2+} current to an increase in NO synthesis; this work suggests involvement of CaM or a CaM-like protein in the signaling cascade. Previous work (e.g., Chiasson et al., 2005) along several different lines has indicated that CaM (or a CaM-like protein) is involved in plant pathogen signaling and the innate immune response, although much is unclear at present regarding what role(s) CaM plays in plant response to pathogens. Speculations include effects on cell redox state, gene expression, phytoalexin synthesis, and mitogen-activated protein kinase pathways and direct involvement in synthesis of ROS (Neill et al., 2002; Ortega et al., 2002; Bouché et al., 2005; Chiasson et al., 2005).

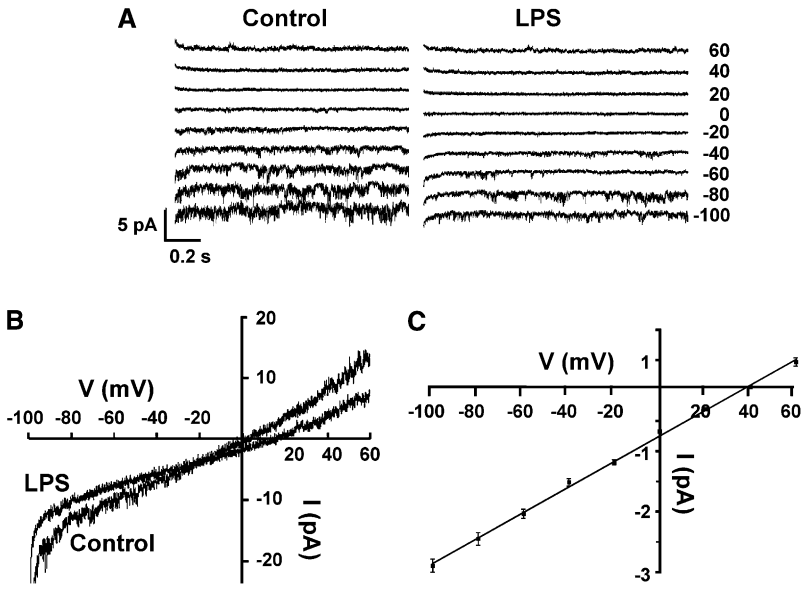

Figure 7. LPS Effects on a Ca^{2+}-Conducting Channel Recorded in the Whole-Cell Configuration from Wild-Type *Arabidopsis* Guard Cell Protoplasts.

(A) Recordings were made at various command potentials (as indicated to the right of the current traces in millivolts) in the absence (Control; left panel) or (at a minimum of) 15 min after addition of 100 μg/mL LPS to the perfusion bath solution (LPS; right panel). Note the single channel events recorded from the guard cell in the absence of LPS. Vertical and horizontal bars represent current and time scales, respectively. Results shown are from one protoplast. Similar results were obtained from a total of three protoplasts in three independent experiments. In the absence of LPS addition to the perfusion bath, the currents recorded at hyperpolarizing voltages did not decrease over the time period used for this experiment (data not shown).

(B) Ramp recordings measured prior to (Control) and >15 min after addition of LPS to the perfusion bath. Ramp currents were recorded from the same protoplast used for the recordings in **(A)**.

(C) Current/voltage relationship generated from the single channel events recorded in the absence of LPS from the experiment shown in **(A)**. Means (±SE) of single channel events recorded at various command potentials are shown. The Nernst equilibrium potential for Ba^{2+} (E_{Ba}) corrected for ionic activity is +41.5 mV; note that the reversal potential calculated for the current (+36 mV) is close to E_{Ba} and far away from E_K (−75 mV) and E_{Cl} (−25 mV), indicating that LPS is inhibiting a Ca^{2+}-conducting channel.

As discussed above, no specific plant gene product has yet been identified as encoding a NOS-type protein. Some studies suggest that plant NOS may have functional and regulatory properties similar to cloned animal NOS proteins (Wendehenne et al., 2001). CaM binds to and activates all animal NOS isoforms (Nedvetsky et al., 2002); in vitro assays of plant NOS activity typically include Ca^{2+}/CaM complex (Planchet et al., 2006). We therefore reasoned that a requirement for Ca^{2+}/CaM (or a CaM-like protein) activation of NOS in planta could provide a mechanism linking CNGC2-dependent plasma membrane inward Ca^{2+} currents (Figure 6) to NO generation in the HR signaling cascade (Figures 1 and 2). Conductance of Ca^{2+} through CNGC2 could lead to a spike of cytosolic Ca^{2+} in plant cells responding to pathogen infection. A rise in the level of Ca^{2+}/CaM could therefore occur downstream from CNGC2 function in a plant innate immunity signaling pathway. The CaM antagonist *N*-(6-aminohexyl)-5-chloro-1-naphthalenesulfonamide (W7) blocks LPS-dependent NO generation in guard cells isolated from either wild-type or *dnd1* plants (cf. Figures 3E and 3G for wild-type cells, see Figure 3H for *dnd1* fluorescence in the presence of W7, and see Figure 2B for *dnd1* fluorescence in the absence of W7). Significantly, the inactive structural analog of W7, *N*-(6-aminohexyl)-1-naphthalenesulfonamide (W5), had no effect on NO generation (cf. Figures 3E and 3F). Thus, these results are consistent with CNGC2-dependent Ca^{2+} conductance leading to NO generation by a rise in cytosolic Ca^{2+}/CaM. We acknowledge the possibility that the antagonist W7 is not specific for CaM but also affects calcium-dependent kinases (e.g., Osuna et al., 2004). The possibility exists, therefore, that calcium-dependent kinases are involved in the signaling pathway linking CNGC2-dependent plasma membrane inward Ca^{2+} currents to NOS-dependent NO generation. However, the most direct explanation for the results shown in Figures 3E to 3G is that W7 prevents CaM activation of NOS in vivo. Further evidence supporting CaM involvement in the plant signaling cascade linking pathogen/PAMP-dependent Ca^{2+} influx to the plant innate immune response involving NO generation and HR is presented in Supplemental Figure 2 online. In addition to W7 blocking the elicitor/PAMP-induced NO generation as shown in Figure 3, we find that the CaM antagonist W7 also prevents HR response to avirulent pathogens (see Supplemental Figure 2 online).

PAMP Activation of CNGC Current

Experiments were undertaken (Figures 7 and 8) to determine if LPS activation of a current could be observed in the same cells in which we demonstrated that LPS activation of NO generation is dependent on inward Ca^{2+} influx through CNGCs (as shown in Figures 2 and 3). In the first series of experiments, whole-cell currents were recorded from guard cell protoplasts ~15 min after addition of LPS to the perfusion bath. In no case (three wild-type *Arabidopsis* protoplasts and three *V. faba* protoplasts, all from different preparations isolated from different plants) did we observe any increase in current at hyperpolarizing potentials after addition of LPS. We did note a modest reduction in current due to LPS; representative currents recorded from one *Arabidopsis* cell are shown in Figure 7. Currents recorded (prior to and >15 min after addition of LPS) at various step voltages are shown in Figure 7A. Ramp recordings are shown for the same cell in Figure 7B.

In a prior study characterizing native CNGC currents in *Arabidopsis* guard cells (Lemtiri-Chlieh and Berkowitz, 2004), we noted that flickery (fast inactivating) inward Ca^{2+}-conducting channel openings can be observed prior to addition of exogenous activating ligand (see also legend of Figure 6 and wild-type recording in absence of added cAMP at −140 to −160 mV); these background currents could be due to endogenous cAMP. A plot (over the linear range of change) of the current/voltage relationship of these single channel openings (from the experiment shown in Figure 7A) is shown in Figure 7C. The reversal potential of the current/voltage relationship (for details, see legend of Figure 7) indicates that the current occurs primarily though a Ca^{2+}-conducting channel.

Prior work from this lab has demonstrated physical binding and a functional interaction between plant CaM isoforms and several plant CNGCs, including CNGC2 (Hua et al., 2003b; Ali

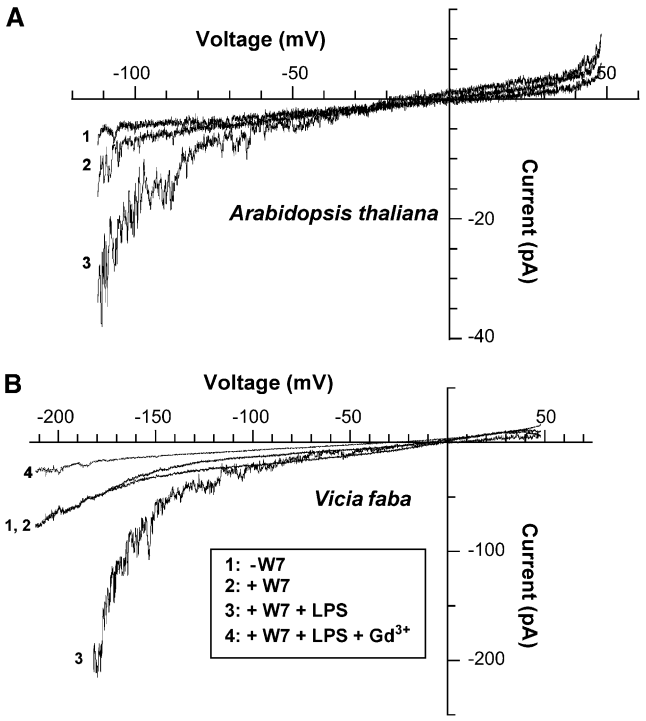

Figure 8. LPS Activates an Inwardly Rectified Ca^{2+} Channel in Guard Cell Protoplasts Preincubated with the CaM Antagonist W7.

Voltage ramps recorded in the whole-cell configuration are shown. Studies were done with wild-type *Arabidopsis* **(A)** or *V. faba* **(B)** guard cell protoplasts.

(A) Recordings were made in standard perfusion buffer (see Methods) (trace 1), with 50 μM W7 added (trace 2), and after addition of 100 μg/mL LPS and 50 μM W7 to the perfusion bath (trace 3). Trace 1 was recorded prior to addition of W7. For the W7 + LPS treatment (trace 3), the protoplast was preincubated for >20 min in W7 prior to adding LPS to the perfusion bath.

(B) Voltage ramps recorded from a *V. faba* guard cell protoplast under similar conditions (traces 1 to 3) as described above **(A)** for *Arabidopsis*. In this experiment, a ramp recording was also made in the presence of W7, LPS, and 50 μM Gd^{3+} (trace 4). Recordings were made from three different *V. faba* protoplasts; representative results from one cell are shown.

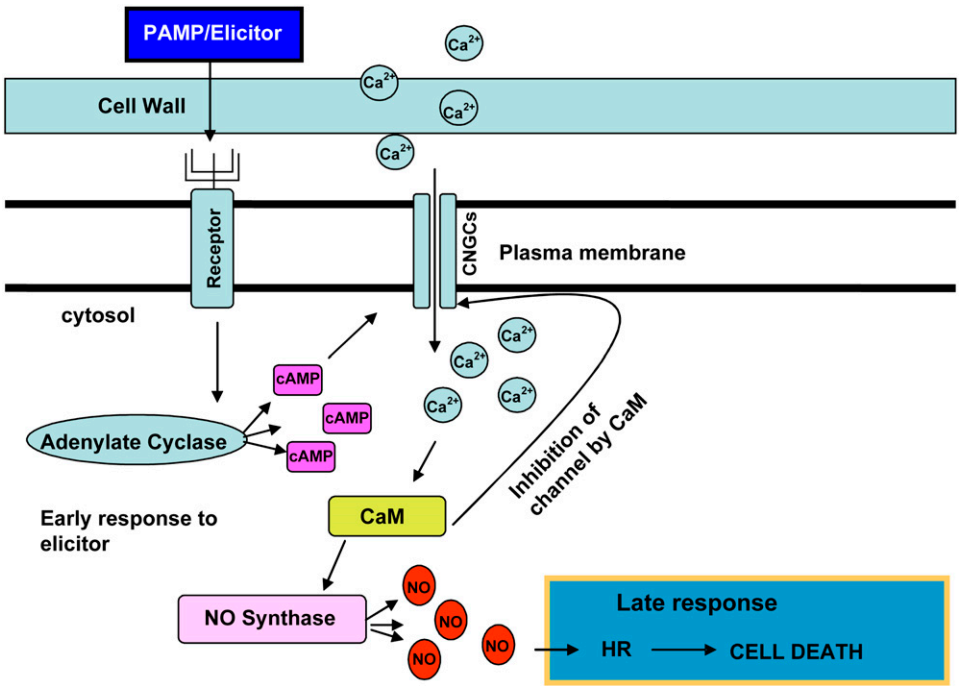

Figure 9. Model of Proposed Early Events in Plant Innate Immune Response/HR to Avirulent Pathogen and/or LPS.

(1) The presence of an extracellular PAMP/elicitor is recognized by an (unknown) receptor in the plant cell plasma membrane. (2) Pathogen/PAMP elicitor recognition by a receptor activates CNGC2 current (either by an increase in cytosolic level of activating ligand through the upregulation of a nucleotide triphosphate cyclase or by some other unknown mechanism). (3) Activation of inward CNGC2 current results in a (transient) increase in cytosolic Ca^{2+}. (4) Cytosolic Ca^{2+}/CaM level increases due to influx of Ca^{2+} into the cell. (5) Ca^{2+}/CaM rise in cytosol inhibits CNGC2, ending the transient cytosolic Ca^{2+} spike. (6) Ca^{2+}/CaM rise activates NOS, leading to an increase in NO generation. (7) NO generation, in concert with other required factors (e.g., presence of the avirulent pathogen), can lead to HR, innate immunity signaling, and, perhaps, diffusion of a signal (NO) to neighboring cells that could result in further CNGC activation (NO is thought to enhance plant cell cytosolic nucleotide triphosphate cyclase activity).

et al., 2006). Application of CaM (in the presence of free cytosolic Ca^{2+}) to the cytosolic side of the channel (expressed in human embryonic kidney cells) inhibited cyclic nucleotide-activated inward current through CNGC2 (Hua et al., 2003b). Based on these results, we speculate that the same (presumed) rise in Ca^{2+}/CaM after application of LPS that activates NOS (i.e., see Figures 3E to 3G) may prevent us from observing a sustained increase in the guard cell Ca^{2+} current as shown in Figure 7. Perhaps the activation of NO by LPS may require just a spike in cytosolic Ca^{2+} rise that could be facilitated by temporary opening of a CNGC; sustained opening of the CNGC during signal transduction could be prevented by CaM block.

In another series of experiments, we monitored LPS effects on currents of guard cell protoplasts that had been first incubated in the CaM antagonist W7 (prior to addition of LPS to the perfusion bath). As shown in Figure 8A, preincubation of *Arabidopsis* guard cell protoplasts in W7 results in an increase of an inwardly rectified, hyperpolarization-activated current upon addition of LPS to the perfusion medium. For example, current at −100 mV in the presence of W7 alone was −7.2 pA, and in the presence of W7 and LPS (i.e., LPS is added after preincubation in W7 for 20 min), current increased to −32.5 mV, a level of current 450% of the level measured with W7 but in the absence of LPS. In a second cell (data not shown), the current at −100 mV was −26 pA in the presence of W7 and LPS. When CaM action is first blocked in *Arabidopsis* guard cell protoplasts by preincubation in W7, addition of LPS to the perfusion medium results in an increase in the measured current.

As mentioned above, we observed no increase in current upon LPS addition to *V. faba* guard cell protoplasts in the absence of W7 (data not shown), and results were similar to those shown for *Arabidopsis* in Figure 7. In the experiment shown in Figure 8B, we evaluated effects of LPS on *V. faba* guard cell protoplasts preincubated in W7. In a fashion similar to results with *Arabidopsis*, we see activation of current upon addition of LPS when protoplasts are preincubated in W7. For example, at −140 mV, the mean (±SE) current recorded from three *V. faba* cells (including the one shown in Figure 8B) was −31.7 ± 12.1 pA in the presence of W7 alone and increased to −80.3 ± 10.1 pA in the presence of W7 and LPS. Application of Gd^{3+} to the perfusion medium along with LPS and W7 completely blocked the current in this experiment, suggesting that LPS activates a Ca^{2+}-conducting channel.

Presumably, W7 prevents Ca^{2+}/CaM block of CNGC2, which could occur as cytosolic Ca^{2+} rises in response to LPS activation

of CNGC2. Consistent with this point, note the difference between the −W7 and +W7 tracings shown in Figure 8A for *Arabidopsis*. With *V. faba* guard cell protoplasts, there was no apparent difference in current at hyperpolarizing voltages in the presence and absence of W7 (Figure 8B). Perhaps the endogenous levels of the secondary messenger molecules CaM and cAMP are not the same in *Arabidopsis* and *V. faba*.

The fact that we are able to observe an increase in inward current at hyperpolarizing voltages upon addition of LPS (instead of reduction of current) when *Arabidopsis* protoplasts are preincubated in W7 is consistent with our conclusion from the work shown in Figure 7 (i.e., that the inhibitory effect of CaM on CNGCs may prevent a sustained increase in current when LPS is added to the perfusion bath in the absence of W7). When CaM action is first blocked in guard cell protoplasts by preincubation in W7, addition of LPS to the perfusion medium now results in an increase in the measured current (Figure 8). In these series of experiments with *Arabidopsis* and *V. faba* guard cell protoplasts, we noted no increase in current in a total of six protoplasts tested when LPS was added without prior exposure to W7 and an increase in current in a total of five (out of five tested) protoplasts when LPS is added after a preincubation in W7.

The results of the experiments in Figure 8 provide preliminary evidence that when the action of CaM in the cytosol is blocked (i.e., in the presence of W7), a Ca^{2+}-conducting channel is activated in response to LPS. These results are consistent with activation of CNGC2 by the pathogen PAMP/elicitor LPS. We acknowledge that direct and definitive evidence supporting this conclusion would be generated by demonstration of a lack of LPS-activated current in *dnd1* guard cell protoplasts preincubated in W7 for >20 min, as was done with protoplasts isolated from wild-type plants in the experiments shown in Figure 8. However, results in Figures 7 and 8 provide indirect evidence consistent with LPS activation of a CNGC current. Sustained LPS activation of the inward cation current occurs only in the presence of W7. The most straightforward explanation for this observation is that the LPS-responsive channel is blocked by CaM (or a CaM-like protein). Of all the known plant ion channels, only CNGCs have a CaM binding domain; they would be the only candidates for channels directly modulated by CaM. An alternative explanation for the results shown in Figures 7 and 8 could be that W7 allows for LPS activation of a Ca^{2+} current by preventing a Ca^{2+}- or Ca^{2+}/CaM-activated protein kinase (i.e., alternative protein targets of W7 other than CaM or a CaM-like protein) from inhibiting an ion channel. To our knowledge, no evidence has yet been published showing block of a plant Ca^{2+}-conducting channel by any Ca^{2+}- or Ca^{2+}/CaM-activated protein kinase; hence, there is no experimental evidence supporting this alternative explanation for results shown in Figures 7 and 8.

Our results (along with the prior studies from this lab; Hua et al., 2003b; Ali et al., 2006) demonstrating CaM block of CNGCs suggest that PAMP presence outside the cell could eventually result in a subsequent block of the channel due to the same buildup of cytosolic Ca^{2+}/CaM that leads to an activation of NOS and NO generation in the innate immunity signaling pathway in a plant cell responding to pathogen infection. We offer no evidence identifying the mechanism by which LPS activates the Ca^{2+} current. However, we speculate that LPS effects on the CNGC2-dependent current may occur by activation of a nucleotide triphosphate cyclase in the cytoplasm, thus leading to an increase in the ligand that activates the channel (Figure 6).

Summary: Development of a New Model of Early Steps in the HR/Innate Immunity Signal Cascade

Work presented here provides new information about plant Ca^{2+}-conducting ion channels, their role in innate immune response to pathogens and the HR signaling cascade, and the involvement of NO in this signaling cascade. Specific conclusions supported by the presented data are as follows. (1) *Arabidopsis* CNGCs function in the native plant plasma membrane. We show evidence that native CNGC2 is a plasma membrane–localized channel protein (i.e., note the difference in whole-cell currents present in wild-type and *dnd1* guard cell protoplasts shown in Figure 6). (2) CNGC gene products (as shown here with CNGC2) function in the plant as cell plasma membrane Ca^{2+} channels (Figure 6). (3) Plasma membrane inward Ca^{2+} currents are linked to NO generation in vivo (Figures 2 to 5) and HR in planta during innate immunity signal cascades (Figure 5; see Supplemental Figures 1 and 2 online) by increases in cytosolic levels of Ca^{2+}/CaM. (Of course, this assertion about plasma membrane Ca^{2+} current involvement in cytosolic Ca^{2+} rise and downstream signaling does not preclude the likely contribution of Ca^{2+}-activated Ca^{2+} channels in the tonoplast contributing to Ca^{2+} spikes during signal cascades [Lamotte et al., 2004; Peiter et al., 2005; Sokolovski et al., 2005].) (4) LPS application to plant cells induces NO generation through the activation of CNGC2 inward Ca^{2+} current (Figures 3, 6, and 8). (5) The presence of a plasma membrane Ca^{2+} channel blocker prevents (the HR component of) innate immunity signaling in response to infection by an avirulent pathogen within the intact plant (Figure 5; see Supplemental Figure 1 online). (6) NO is required for HR. Our work with SNP and HR in the *dnd1* mutant (Figure 1) suggests that NO is required but not sufficient alone (i.e., in the absence of a pathogen) to initiate an HR response in *Arabidopsis*. The aforementioned conclusions about the interplay of Ca^{2+} conductance through plasma membrane CNGC2, NO, and the cytosolic secondary messengers cyclic nucleotide, CaM, and Ca^{2+} in early events of PAMP/pathogen perception signaling cascades in plants are summarized in the model presented in Figure 9.

METHODS

Plant Material

Vicia faba (New England Seed Co.) or *Arabidopsis thaliana* wild-type (Columbia ecotype) and *dnd1* (Clough et al., 2000) plants were grown in a growth chamber on LP5 potting mix containing starter fertilizer (Sun Gro) at 12 h light (100 μE)/12 h dark (except where noted in figure legends) and 21°C. After 3 weeks of growth in flats, *Arabidopsis* seedlings were transplanted into pots containing the same mix. As characterized by Clough et al. (2000), the *dnd1 Arabidopsis* genotype is homozygous for a null mutation in the gene (At5g15410) encoding CNGC2. The *dnd1* allele contains a G-to-A point mutation that creates a stop codon in exon 3 at Trp290, generating a severely truncated and nonfunctional CNGC2 coding sequence. *V. faba* plants were used after 4 to 6 weeks of growth.

Nicotiana tabacum plants were grown in potting mx in a greenhouse under ambient conditions with supplemental lighting (mercury halide lamps); fully expanded nonsenescing leaves were used.

HR Evaluation

Wild-type and *dnd1 Arabidopsis* plants were grown on LP5 potting mix (as above) for 6 to 7 weeks. Plants were then irrigated with half-strength Murashige and Skoog medium with or without 100 μM SNP twice a week for 2 more weeks prior to infection with *Pseudomonas syringae*. Our use of SNP applied to growing medium as a NO donor to plants follows the strategy used by Guo et al. (2003) to revert some (*At noa1*) mutant phenotypes associated with low leaf NO to the wild type. As a control, Guo et al. (2003) demonstrated that application of sodium ferrocyanide, an SNP analog that does not release NO (but generates the SNP breakdown product cyanide), had no effect on their phenotype. Modolo et al. (2002) and Zhao et al. (2006) demonstrated that sodium ferrocyanide did not reproduce the effect of SNP application on a NO-related phenotype as well. He et al. (2004) demonstrated that SNP application mimicked some NO-related phenotypes displayed by an *Arabidopsis* mutant that has constitutively high endogenous NO. Like Guo et al. (2003), Graziano et al. (2002) supplied SNP to the growing medium of plants through the irrigation water and similarly demonstrated complementation of some NO-dependent plant phenotypes. Significantly, Graziano et al. (2002) duplicated SNP irrigation treatment effects on the plant with supply of gaseous NO in a growth chamber and also by treatment with *S*-nitroso-*N*-acetylpenicillamine, an SNP analog that does not generate cyanide as a breakdown product. They also demonstrated NO release by the SNP treatment in their work. We can presume from recent studies (Floryszak-Wieczorek et al., 2006) that NO release into the growth chamber atmosphere occurs from the SNP-irrigated growth medium. The aforementioned studies provide an experimental basis for our strategy of treating plants with this NO donor.

P. syringae pv *syringae* strain 61 (*Pss*) and *P. syringae* pv *tomato* (DC3000) (*Pst*) were used for the experiments shown in this report (pathovars are noted in figure legends). In the case of *Pst*, *avrRpt2*$^+$, *avrRpt2*$^-$, *avrRpm1*$^+$, or *avrRpm1*$^-$ strains were used. Avirulence of the *Pss* pathogen strain on wild-type *Arabidopsis* has been demonstrated previously (Losada et al., 2004). Unless stated otherwise, all chemicals were from Sigma-Aldrich. Bacteria were cultured in Luria-Bertani medium (10 g/L tryptone, 5 g/L yeast extract, 5 g/L NaCl, pH 7.0, and 100 μg/mL rifampicin) overnight at 28°C, washed once in 10 mM $MgCl_2 \cdot 6H_2O$, and resuspended at 2×10^8 colony-forming units/mL (for *Pss*) or 5×10^6 (for DC3000) in 10 mM $MgCl_2 \cdot 6H_2O$. For some experiments, other concentrations of inoculum were used; titers are noted in figure legends. Interveinal regions of the abaxial surface of fully mature, nonsenescing leaves of plants were inoculated by syringe injection (Katagiri et al., 2002). A 1-mL blunt-end syringe was used to deliver inoculum to the intercellular subcuticular space. HR symptoms were scored (one to six, with six representing 100% tissue collapse with tissue browning) 24 h after infection as described by Jackson et al. (1999). HR-related tissue necrosis was also evaluated after incubation of leaves detached from plants (time after infection noted in figure legends) in ethanol with gentle shaking for a minimum of 3 (*Arabidopsis*) or 7 (*V. faba*) d. When autofluorescence of leaf tissue was monitored prior to ethanol bleaching, images were captured using an inverted Olympus IX70 microscope and green fluorescence protein excitation and emission filters. Digitized images were acquired using a MagnaFire CCD camera and software (Optronics).

In Vivo NO Analysis

NO was measured in guard cells of leaf epidermal peels prepared from leaves of 6-week-old wild-type and *dnd1* plants (grown as described above) using DAF-2DA fluorescence as described by Guo et al. (2003) with the following modifications. The epidermal peels were stained in loading buffer (5 mM MES-KOH, 0.25 mM KCl, and 1 mM $CaCl_2$, pH 5.7) containing 50 μM DAF-2DA and then washed three times with buffer alone. After dye loading and washing, the peels were incubated for 15 to 20 min in Sigma-Aldrich NOS assay kit reaction buffer with additions as noted in figure legends. Peels were transferred either to reaction buffer containing 100 μg/mL *Pseudomonas aeruginosa* phenol-extracted LPS (or buffer control) or preincubated for 5 to 10 min first in reaction buffer containing inhibitors/ligands as follows: 50 μM SNP, 200 μM L-NAME or D-NAME, 50 μM W7 or W5, 2 mM Na_2EGTA, 10 mM TEA, or 100 μM $GdCl_3$. When peels containing guard cells were incubated with these compounds, they were then transferred to reaction mix containing reaction buffer, 100 μg/mL LPS, and with or without the specific compounds as indicated in the figures. The epidermal peels were placed underneath a cover slip on a microscope slide with several drops of reaction mix. NO-dependent DAF-2DA fluorescence was monitored over time; for each treatment, images show the maximum fluorescence intensity. NO-dependent DAF-2DA fluorescence and bright-field images were captured using an inverted Olympus IX70 microscope and green fluorescence protein excitation and emission filters. Digitized images were acquired using a MagnaFire CCD camera and software.

We note that LPS preparations can be contaminated with other bacterial components that can affect cell immune responses (Zeidler et al., 2004). Relevant to the work in this report, Zeidler et al. (2004) have shown that the LPS prepared from 15 different bacteria (including the *P. aeruginosa* LPS we used) prepared using a range of methods all similarly induced NO in *Arabidopsis* cells. As indicated above, work shown in this report was done with phenol-extracted LPS. However, we repeated some key experiments with phenol-extracted LPS further purified using Sepharose gel filtration and found similar results as those reported in Figures 2 and 3 (data not shown). In addition, we found that our LPS induction of NO in intact guard cells in epidermal peels could be reproduced using a peptide PAMP from a plant fungal pathogen (data not shown). These points support our use of our LPS preparations as a PAMP.

Quantitative analysis of DAF-2DA fluorescence was undertaken using ImageJ processing/analysis software developed from NIH Image (Abramoff et al., 2004) available at http://rsb.info.nih.gov/ij/download.html. The digitized image showing maximum fluorescence for a guard cell pair from an epidermal peel represented a treatment replicate; a minimum of three epidermal peels were analyzed as replicates for each treatment. In many cases, a digital image captured more than one guard cell pair at maximal fluorescence intensity (the average number of guard cell pairs analyzed for an individual replicate was approximately three). When more than one guard cell pair was analyzed for a replicate, the fluorescence intensities for the guard cell pairs in the image were averaged and that value used as a single treatment replicate. For analysis of fluorescence intensity of an individual guard cell pair, the bright-field and fluorescence images of an epidermal peel were stacked in the ImageJ program (allowing for a guard cell pair to be identified and size-expanded within the field of view and its area highlighted in the fluorescent image even if the field was completely dark). Brightness of the selected fluorescence image was recorded within the defined range of 256 shades of gray per unit area averaged over the entire region of the guard cell pair. In many cases, the control treatment fluorescence intensities were overexposed (i.e., reaching 256 arbitrary light units/pixel over the region of the guard cell pair) (see Figure 4). Therefore, the quantitative analysis of NO generation in epidermal peels presented in this work is likely an underestimation of differences between the treatments.

Electrophysiology

Guard cell protoplasts were isolated from leaves of 5- to 6-week-old *Arabidopsis* or 3-week-old *V. faba* plants exactly as described previously (Lemtiri-Chlieh et al., 2003; Lemtiri-Chlieh and Berkowitz, 2004). After

enzymatic digestion of abaxial epidermal peels of leaf tissue and centrifugation purification, guard cells were kept on ice in 1 to 2 mL of medium containing 0.42 M mannitol, 10 mM MES, 200 μM $CaCl_2$, 2.5 mM KOH (pH 5.5 and osmolality at 466 mOsm/kg) and used for patch clamp recordings for several hours after isolation. Whole-cell recordings of I_{Ca} were obtained as described (Lemtiri-Chlieh and Berkowitz, 2004). Protoplasts were placed in an ~0.4-mL recording chamber, allowed to settle, and then perfused continuously at flow rates of ~0.5 mL/min with a bath solution containing 50 mM $BaCl_2$, 1 mM KCl, and 10 mM MES-KOH, pH 5.5, an osmolality adjusted to 470 mOsm/kg using mannitol, and with additions as noted in the figures. The perfusion system in all our experiments was gravity driven (~0.5 mL/min; it takes several minutes for the ligand to reach the recording chamber via the tubing). The flow rate is about one chamber volume per minute.

Patch pipettes (5 to 10 μm) contained 5 mM $BaCl_2$, 20 mM KCl, and 10 mM HEPES-KOH, pH 7.5, with an osmolality adjusted to 500 mOsm/kg with mannitol. Experiments were performed at room temperature (20 to 22°C) using standard whole-cell patch clamp techniques, with an Axopatch 200B Integrating Patch Clamp amplifier (Axon Instruments). Voltage commands and simultaneous signal recordings and analyses were assessed by a microcomputer connected to the amplifier via a multipurpose input/output device (Digidata 1320A) using pClamp 9.0 software (Axon Instruments). All current traces shown were low-pass filtered at 2 kHz before analog-to-digital conversion and were uncorrected for leakage current or capacitive transients. Membrane potentials were corrected for liquid junction potential.

After giga-ohm seals were formed in a cell-attached configuration, the whole-cell configuration was achieved by gentle suction, and the membrane was immediately clamped to a holding potential of −30 mV. Protoplasts were perfused for a minimum of 3 to 5 min prior to initiating any recordings. Whole-cell recordings were made using ramp (typically 200 mV ramps over 2 s) or gap-free protocols with the membrane clamped to various command voltages (as indicated in the figures). All individual recordings shown and/or mentioned in this report were undertaken on guard cell protoplasts isolated from different plants (i.e., each individual recording was made on protoplasts from different preparations).

The lipophilic cAMP analog dibutyryl-cAMP (db-cAMP) was solubilized in deionized water and stored in aliquots of 50 to 100 μL at a concentration of 0.1 M. A few minutes before the experiment, db-cAMP solutions were diluted to the final desired concentration. Recordings of cAMP-activated current presented in this work were made after exposure of protoplasts to activating ligand for many minutes (~10 min or more).

It should be noted that cyclic nucleotide typically activates animal CNGCs in native membranes within seconds. In our studies of native cyclic nucleotide activated current in plant cells (also see Lemtiri-Chlieh and Berkowitz, 2004), we typically see ligand activation of current in the whole-cell configuration many minutes after addition of cyclic nucleotide to the perfusion medium. Alternatively, prior work from this lab has demonstrated activation of plant CNGCs within seconds after exposure to ligand when recordings are made in the patch configuration. We speculate that the long incubation times required for ligand activation in the whole-cell configuration could be due to either of two possibilities. (1) CaM binds to animal CNGCs at the N terminus, while the cyclic nucleotide binding domain is at the C terminus; the effect of CaM is allosteric (Trudeau and Zagotta, 2004). With plant CNGCs, the two binding domains are both at the C terminus; they physically and functionally overlap (Hua et al., 2003b; Ali et al., 2006). Clearly, the molecular mechanism mediating CaM block of ligand activation in plant and animal CNGCs is different. Therefore, projections about ligand activation from animal CNGCs to the plant homologs should be made with caution; they are dissimilar proteins in this particular respect. Perhaps it takes many minutes for the exogenously added activating ligand to compete with bound CaM (present in the cytoplasm of protoplasts but diffused away from membrane patches). (2) Another explanation for the long activation times is the possibility that plant cells have relatively higher levels of cyclic nucleotide phosphodiesterases than animal cells; the lower ambient levels of cyclic nucleotides in plant cells is consistent with this possibility (Newton and Smith, 2004). Perhaps, high phosphodiesterase activity present in the plant cytoplasm necessitates long incubation times (required for buildup of ligand concentration) when channels are activated within the milieu of the intact cytoplasm. To out knowledge, no one has yet published results showing ligand activation of plant CNGCs in intact protoplasts over shorter time periods than reported here.

Accession Numbers

The Arabidopsis Genome Initiative locus identifier numbers for the genes mentioned in this article are At5g15410 (*CNGC2*) and At3g47450 (At *NOS1/NOA1*).

Supplemental Data

The following materials are available in the online version of this article.

Supplemental Figure 1. Gd^{3+} Effects on Growth of *P. syringae* Cultured on Solid Medium and on Pathogen-Related Necrosis in *V. faba* and *N. tabacum*.

Supplemental Figure 2. The CaM Antagonist W7 Prevents Pathogen-Related Necrosis in Planta.

ACKNOWLEDGMENTS

The work described in this report was supported by National Science Foundation Awards MCB-0344141 to G.A.B and MCB-0211687 to S.v.B. We thank Steven Hutcheson for the gift of *P. syringae* pv *syringae*. We thank Andries Smigel for technical assistance and Debra Norris for assistance with image analysis. We also thank Jeffrey Dangl for the gift of *P. syringae* pv *tomato avrRpm1*, Walter Gassmann for the gift of *P. syringae* pv *tomato avrRpt2*, and both of these eminent scientists for helpful discussions and advice regarding the work described in this report.

Received June 20, 2006; revised February 9, 2007; accepted March 5, 2007; published March 23, 2007.

REFERENCES

Abramoff, M.D., Magelhaes, P.J., and Ram, S.J. (2004). Image processing with ImageJ. Biophotonics International **11:** 36–42.

Ali, R., Zielinski, R., and Berkowitz, G.A. (2006). Expression of plant cyclic nucleotide-gated cation channels in yeast. J. Exp. Bot. **57:** 125–138.

Balagué, C., Lin, B., Alcon, C., Flottes, G., Malmström, S., Köhler, C., Neuhaus, G., Pelletier, G., Gaymard, F., and Roby, D. (2003). HLM1, and essential signaling component in the hypersensitive response, is a member of the cyclic nucleotide-gated channel ion channel family. Plant Cell **15:** 365–379.

Bindschedler, L.V., Minibayeva, F., Gardner, S.L., Gerrish, C., Davies, D.R., and Bolwell, G.P. (2001). Early signalling events in the apoplastic oxidative burst in suspension cultured French bean cells involve cAMP and Ca^{2+}. New Phytol. **151:** 185–194.

Bouché, N., Yellin, A., Snedden, W.A., and Fromm, H. (2005). Plant-specific calmodulin-binding proteins. Annu. Rev. Plant Biol. **56:** 435–466.

Braun, S.G., Meyer, A., Holst, O., Pühler, A., and Niehaus, K. (2005). Characterization of the *Xanthomonas campestris* pv. *campestris* lipopolysaccharide substructures essential for elicitation of an oxidative burst in tobacco cells. Mol. Plant Microbe Interact. **18:** 674–681.

Bright, J., Radhika, D., Hancock, J.T., Weir, I.S., and Neill, J.S. (2006). ABA-induced NO generation and stomatal closure in Arabidopsis are dependent on H_2O_2 synthesis. Plant J. **45:** 113–122.

Chiasson, D., Ekengren, S.K., Martin, G.B., Dobney, S.L., and Snedden, W.A. (2005). Calmodulin-like proteins from Arabidopsis and tomato are involved in host defense against *Pseudomonas syringae* pv. tomato. Plant Mol. Biol. **58:** 887–897.

Clough, S.J., Fengler, K.A., Yu, I.C., Lippok, B., Smith, R.K., Jr., and Bent, A.F. (2000). The Arabidopsis dnd1 ''defense, no death'' gene encodes a mutated cyclic nucleotide-gated ion channel. Proc. Natl. Acad. Sci. USA **97:** 9323–9328.

Crawford, N.M., Galli, M., Tischner, R., Heimer, Y.M., Okamoto, M., and Mack, A. (2006). Response to Zemojtel et al: Plant nitric oxide synthase: Back to square one. Trends Plant Sci. **11:** 526–527.

Crawford, N.M., and Guo, R.-Q. (2005). New insights into nitric oxide metabolism and regulatory functions. Trends Plant Sci. **10:** 195–200.

Dangl, J.L. (1998). Innate immunity: Plants just say NO to pathogens. Nature **394:** 525–527.

Dangl, J.L., Dietrich, R.A., and Richberg, M.H. (1996). Death don't have no mercy: Cell death programs in plant-microbe interactions. Plant Cell **8:** 1793–1807.

Delledonne, M. (2005). NO news is good news for plants. Curr. Opin. Plant Biol. **8:** 390–396.

Delledonne, M., Xia, Y., Dixon, R.A., and Lamb, C. (1998). Nitric oxide functions as a signal in plant disease resistance. Nature **394:** 585–588.

Delledonne, M., Zeier, J., Marocco, A., and Lamb, C. (2001). Signal interactions between nitric oxide and reactive oxygen intermediates in the plant hypersensitive disease resistance response. Proc. Natl. Acad. Sci. USA **98:** 13454–13459.

Durner, J., Wendehenne, D., and Klessig, D.F. (1998). Defense gene induction in tobacco by nitric oxide, cyclic GMP, and cyclic ADP-ribose. Proc. Natl. Acad. Sci. USA **95:** 10328–10333.

Floryszak-Wieczorek, J., Milczarek, G., Arasimowicz, M., and Ciszewski, A. (2006). Do nitric oxide donors mimic endogenous NO-related response in plants? Planta **224:** 1363–1372.

Flynn, G.E., Johnson, J.P., and Zagotta, W.N. (2001). Cyclic nucleotide-gated channels: Shedding light on the opening of a channel pore. Nat. Rev. Neurosci. **2:** 643–652.

Gelli, A., and Blumwald, E. (1997). Hyperpolarization-activated Ca^{2+}-permeable channels by race-specific fungal elicitors. J. Membr. Biol. **155:** 35–45.

Grant, M., Brown, I., Adams, S., Knight, M., Ainslie, A., and Mansfield, J. (2000). The *RPM1* plant disease resistance gene facilitates a rapid and sustained increase in cytosolic calcium that is necessary for the oxidative burst and hypersensitive cell death. Plant J. **23:** 441–450.

Graziano, M., Beligni, M.V., and Lamattina, L. (2002). Nitric oxide improves internal iron availability in plants. Plant Physiol. **130:** 1852–1859.

Guo, F.-Q., Okamoto, M., and Crawford, N.M. (2003). Identification of a plant nitric oxide synthase gene involved in hormonal signaling. Science **302:** 100–103.

He, Y., et al. (2004). Nitric oxide represses the Arabidopsis floral transition. Science **305:** 1968–1971.

Hetherington, A.M., and Brownlee, C. (2004). The generation of Ca^{2+} signals in plants. Annu. Rev. Plant Biol. **55:** 401–427.

Hua, B.G., Leng, Q., Mercier, R.W., and Berkowitz, G.A. (2003a). Plants do it differently. A new basis for potassium/sodium selectivity in the pore of an ion channel. Plant Physiol. **132:** 1353–1361.

Hua, B.G., Mercier, R.W., Zielinski, R.E., and Berkowitz, G.A. (2003b). Functional interaction of calmodulin with a plant cyclic nucleotide gated cation channels. Plant Physiol. Biochem. **41:** 945–954.

Jackson, R.W., Athanassopoulos, E., Tsiamis, G., Mansfield, J.W., Sesma, A., Arnold, D.L., Gibbon, M.J., Murillo, J., Taylor, J.D., and Vivian, A. (1999). Identification of a pathogenicity island, which contains genes for virulence and avirulence, on a large native plasmid in the bean pathogen *Pseudomonas syringae* pathovar *phaseolicola*. Proc. Natl. Acad. Sci. USA **96:** 10875–10880.

Katagiri, F., Thilmony, R., and He, S.Y. (March 27, 2002). The *Arabidopsis thaliana-Pseudomonas syringae* interaction. In The Arabidopsis Book, C.R. Somerville and E.M. Meyerowitz, eds (Rockville, MD: American Society of Plant Biologists), doi/10.1199/tab.0039, http://www.aspb.org/publications/arabidopsis/.

Lamotte, O., Courtois, C., Barnavon, L., Pugin, A., and Wendehenne, D. (2005). Nitric oxide in plants: The biosynthesis and cell signaling properties of a fascinating molecule. Planta **221:** 1–4.

Lamotte, O., Gould, K., Lecourieux, D., Sequeira-Legrand, A., Lebrun-Garcia, A., Durner, J., Pugin, A., and Wendehenne, D. (2004). Analysis of nitric oxide signaling functions in tobacco cells challenged by the elicitor cryptogein. Plant Physiol. **135:** 516–529.

Lee, S., Choi, H., Suh, S., Doo, I.-S., Oh, K.-Y., Choi, E.J., Taylor, A.T.S., Low, P.S., and Lee, Y. (1999). Oligogalacturonic acid and chitosan reduce stomatal aperture by inducing the evolution of reactive oxygen species from guard cells of tomato and *Commelina communis*. Plant Physiol. **121:** 147–152.

Lemtiri-Chlieh, F., and Berkowitz, G.A. (2004). Cyclic adenosine monophosphate regulates calcium channels in the plasma membrane of Arabidopsis leaf guard and mesophyll cells. J. Biol. Chem. **279:** 35306–35312.

Lemtiri-Chlieh, F., MacRobbie, E.A.C., Webb, A.A.R., Manison, N.F., Brownlee, C., Skepper, J.N., Chen, J., Prestwitch, G.D., and Brearley, C.A. (2003). Inositol hexakisphosphate mobilizes an endomembrane store of calcium in guard cells. Proc. Natl. Acad. Sci. USA **100:** 10091–10095.

Leng, Q., Mercier, R.W., Hua, B.G., Fromm, H., and Berkowitz, G.A. (2002). Electrophysiological analysis of cloned cyclic nucleotide-gated ion channels. Plant Physiol. **128:** 400–408.

Leng, Q., Mercier, R.W., Yao, W.Z., and Berkowitz, G.A. (1999). Cloning and first functional characterization of a plant cyclic nucleotide-gated cation channel. Plant Physiol. **121:** 753–761.

López-Solanilla, E., Bronstein, P.A., Schneider, A.R., and Collmer, A. (2004). HopPtoN is a *Pseudomonas syringae* Hrp (type III secretion system) cysteine protease effector that suppresses pathogen-induced necrosis associated with both compatible and incompatible plant interactions. Mol. Microbiol. **54:** 353–365.

Losada, L., Sussan, T., Pak, K., Zeyad, S., Rozenbaum, I., and Hutcheson, S.W. (2004). Identification of a novel *Pseudomanas syringae* Psy61 effector with virulence and avirulence functions by a HrpL-dependent promoter-trap assay. Mol. Plant Microbe Interact. **17:** 254–262.

Modolo, L.V., Cunha, F.Q., Braga, M.R., and Salgado, I. (2002). Nitric oxide synthase-mediated phytoalexin accumulation in soybean cotyledons in response to the *Diaporthe phaseolorum* f. sp. *meridionalis* elicitor. Plant Physiol. **130:** 1288–1297.

Nedvetsky, P.I., Sessa, W.C., and Schmidt, H.H. (2002). There's NO binding like NOS binding: Protein–protein interactions in NO_cGMP signaling. Proc. Natl. Acad. Sci. USA **99:** 16510–16512.

Neill, S.J., Desikan, R., Clarke, A., Hurst, R.D., and Hancock, J.T. (2002). Hydrogen peroxide and nitric oxide as signalling molecules in plants. J. Exp. Bot. **53:** 1237–1247.

Newman, M.A., von Roepenack-Lahaye, E., Parr, A., Daniels, M.J., and Dow, J.M. (2002). Prior exposure to lipopolysaccharide potentiates

expression of plant defenses in response to bacteria. Plant J. **29:** 487–495.

Newton, R.P., and Smith, C.J. (2004). Cyclic nucleotides. Phytochemistry **65:** 2423–2437.

Nürnberger, T., Brunner, F., Kemmerling, B., and Piater, L. (2004). Innate immunity in plants and animals: Striking similarities and obvious differences. Immunol. Rev. **198:** 249–266.

Ortega, X., Polanco, R., Castaneda, P., and Perez, L.M. (2002). Signal transduction in lemon seedlings in the hypersensitive response against *Alternaria alternata*: Participation of calmodulin, G-protein and protein kinases. Biol. Res. **35:** 373–383.

Osuna, L., Coursol, S., Pierre, J.N., and Vidal, J. (2004). A Ca($^{2+}$)-dependent protein kinase with characteristics of protein kinase C in leaves and mesophyll cell protoplasts from *Digitaria sanguinalis*: Possible involvement in the C(4)-phosphoenolpyruvate carboxylase phosphorylation cascade. Biochem. Biophys. Res. Commun. **314:** 428–433.

Peiter, E., Maathuis, F.J.M., Mills, L.N., Knight, H., Pelloux, J., Hetherington, A.M., and Sanders, D. (2005). The vacuolar Ca^{2+}-activated channel TPC1 regulates germination and stomatal movement. Nature **434:** 404–408.

Peng, S.-Q., Hajela, R.K., and Atchison, W.D. (2005). Fluid flow-induced increase in inward Ba^{2+} current expressed in HEK293 cells transiently transfected with human neuronal L-type Ca^{2+} channels. Brain Res. **1045:** 116–123.

Planchet, E., and Kaiser, W.M. (2006). Nitric oxide (NO) detection by DAF fluorescence and chemiluminescence: A comparison using abiotic and biotic NO sources. J. Exp. Bot. **57:** 3043–3055.

Planchet, E., Sonoda, M., Zeier, J., and Kaiser, W.M. (2006). Nitric oxide (NO) as an intermediate in the cryptogein-induced hypersensitive response – A critical re-evaluation. Plant Cell Environ. **29:** 59–69.

Romero-Puertas, M.C., Perazzolli, M., Zago, E.D., and Delledonne, M. (2004). Nitric oxide signaling functions in plant-pathogen interactions. Cell. Microbiol. **6:** 795–803.

Schornack, S., Ballvora, A., Gurlebeck, D., Peart, J., Baulcombe, D., Ganal, M., Baker, B., Bonas, U., and Lahaye, T. (2004). The tomato resistance protein Bs4 is a predicted non-nuclear TIR-NB-LRR protein that mediates defense responses to severely truncated derivatives of AvrBs4 and overexpressed AvrBs3. Plant J. **37:** 46–60.

Sokolovski, S., Hills, A., Gay, R., Garcia-Mata, C., Lamattina, L., and Blatt, M.R. (2005). Protein phosphorylation is a prerequisite for intracellular Ca^{2+} release and ion channel control by nitric oxide and abscisic acid in guard cells. Plant J. **43:** 520–529.

Talke, I.N., Blaudez, D., Maathuis, F.J.M., and Sanders, D. (2003). CNGCs: Prime targets of plant cyclic nucleotide signalling? Trends Plant Sci. **8:** 286–293.

Torres, M.A., Jones, J.D.G., and Dangl, J.L. (2006). Reactive oxygen species signaling in response to pathogens. Plant Physiol. **141:** 373–378.

Trudeau, M.C., and Zagotta, W.N. (2004). Dynamics of Ca^{2+}-calmodulin-independent inhibition of rod cyclic nucleotide-gated channels measured by patch-clamp fluorometry. J. Gen. Physiol. **124:** 211–223.

Weber, E., Ojanen-Reuhs, T., Huguet, E., Hause, G., Romantschuk, M., Korhonen, T.K., Bonas, U., and Koebnik, R. (2005). The type III-dependent Hrp pilus is required for productive interaction of *Xanthomonas campestris* pv. *vesicatoria* with pepper host plants. J. Bacteriol. **187:** 2458–2468.

Wendehenne, D., Durner, J., and Klessig, D.F. (2004). Nitric oxide: A new player in plant signalling and defense responses. Curr. Opin. Plant Biol. **7:** 449–455.

Wendehenne, D., Pugin, A., Klessig, D.F., and Durner, J. (2001). Nitric oxide: Comparative synthesis and signaling in animal and plant cells. Trends Plant Sci. **6:** 177–183.

White, P.J., Bowen, H.C., Demidchik, V., Nichols, C., and Davies, J.M. (2002). Genes for calcium-permeable channels in the plasma membrane of plant root cells. Biochim. Biophys. Acta **1564:** 299–309.

White, P.J., and Broadley, M.R. (2003). Calcium in plants. Ann. Bot. (Lond.) **92:** 487–511.

Wright, K.M., Duncan, G.H., Pradel, K.S., Carr, F., Wood, S., Oparka, K.J., and Santa Cruz, S. (2000). Analysis of the *N* gene hypersensitive response induced by a fluorescently tagged tobacco mosaic virus. Plant Physiol. **123:** 1375–1385.

Yu, I.C., Parker, J., and Bent, A.F. (1998). Gene-for-gene disease resistance without the hypersensitive response in Arabidopsis dnd1 mutant. Proc. Natl. Acad. Sci. USA **95:** 7819–7824.

Zeidler, D., Zähringer, U., Gerber, I., Dubery, I., Hartung, T., Bors, W., Jutzler, P., and Durner, J. (2004). Innate immunity and *Arabidopsis thaliana*: Lipopolysaccharides activate nitric oxide synthase (NOS) and induce defense genes. Proc. Natl. Acad. Sci. USA **101:** 15811–15816.

Zemojtel, T., Frohlich, A., Palmieri, M.C., Kolanczyk, M., Mikula, I., Wyrwicz, L.S., Wanker, E.E., Mundlos, S., Vingron, M., Martasek, P., and Durner, J. (2006). Plant nitric oxide synthase: A never-ending story? Trends Plant Sci. **11:** 524–525.

Zhang, C., Czymmek, K.J., and Shapiro, A.D. (2003). Nitric oxide does not trigger early programmed cell death events but may contribute to cell-to-cell signaling governing progression of the Arabidopsis hypersensitive response. Mol. Plant Microbe Interact. **16:** 962–972.

Zhao, M., Zhao, X., Wu, Y., and Zhang, L. (May 9, 2006). Enhanced sensitivity to oxidative stress in an Arabidopsis nitric oxide synthase mutant. J. Plant Physiol. http://dx.doi.org/10.1016/j.jplph.2006.03.002.

Zheng, J., and Zagotta, W.N. (2004). Stoichiometry and assembly of olfactory cyclic nucleotide-gated channels. Neuron **42:** 411–421.